Comparison of experimental and theoretical triple differential cross sections for the single ionization of CO_2 ($1\pi_g$) by electron impact

Zehra N. Ozer,[1,*] Esam Ali,[2] Mevlut Dogan,[1] Murat Yavuz,[1] Osman Alwan,[3,4] Adnan Naja,[3] Ochbadrakh Chuluunbaatar,[5] Boghos B. Joulakian,[4] Chuan-Gang Ning,[6] James Colgan,[7] and Don Madison[2]

[1]*Department of Physics, e-COL Laboratory, Afyon Kocatepe University, 03200, Afyon, Turkey*

[2]*Department of Physics, Missouri University of Science and Technology, Rolla, Missouri 65409, USA*

[3]*Lebanese University, LPM, EDST, Tripoli 1300, Lebanon*

[4]*Universitè de Lorraine, SRSMC (UMR CNRS 7565), 1 Bld. Arago, Bat. ICPM 57078 Metz Cedex 3, France*

[5]*Joint Institute for Nuclear Research, Dubna, Moscow Region 141980, Russia*

[6]*Department of Physics, State Key Laboratory of Low-Dimensional Quantum Physics, Tsinghua University, Beijing 100084, China*

[7]*Theoretical Division, Los Alamos National Laboratory, Los Alamos, New Mexico 87545, USA*

(Received 10 February 2016; revised manuscript received 1 April 2016; published 20 June 2016)

Experimental and theoretical triple differential cross sections for intermediate-energy (250 eV) electron-impact single ionization of the CO_2 are presented for three fixed projectile scattering angles. Results are presented for ionization of the outermost $1\pi_g$ molecular orbital of CO_2 in a coplanar asymmetric geometry. The experimental data are compared to predictions from the three-center Coulomb continuum approximation for triatomic targets, and the molecular three-body distorted wave (M3DW) model. It is observed that while both theories are in reasonable qualitative agreement with experiment, the M3DW is in the best overall agreement with experiment.

DOI: 10.1103/PhysRevA.93.062707

I. INTRODUCTION

Electron-impact single ionization of molecules is of interest not only due to practical applications, but also due to obtaining a better understanding of fundamental physics. On the practical application side, studies of electron-impact ionization of atmospheric molecules are useful for controlling and monitoring global warming. Information on single ionization of atmospheric molecules is also important both for understanding the development of planetary atmospheres and controlling the events in the ionosphere and its neighboring regions.

For a number of reasons, CO_2 is one of the most important gases on Earth. Plants use CO_2 to produce sugars and starches in photosynthesis that are necessary for the survival of life. CO_2 in the atmosphere is also important because it absorbs heat radiated from the Earth's surface, and increasing levels of CO_2 in the atmosphere may be responsible for long-term changes in the Earth's climate.

CO_2 is also an important molecule in applied fields from astrophysics to plasma chemistry, and it is the main component in the atmospheres of Venus and Mars so it is an important molecule to study and understand. Fully differential electron-impact ionization studies, called (e,2e), provide the richest information for understanding the dynamics of the reaction process and also the dynamics of the target for ionization of atoms/molecules. The motivation of this work is to present experimental and theoretical results to further study the dynamics of such reactions. Since CO_2 is a linear triatomic molecule, it is a good starting point which could motivate studies of more complicated polyatomic molecules.

Due to the growing interest in the behavior of this molecule, some reviews have been published for different types of cross sections [1–4]. Several groups have measured the angular distribution of electrons elastically scattered from CO_2 for intermediate [5] and low energies [6,7]. Some works have concentrated on determining the absolute scale of the cross sections [8–10]. Comprehensive sets of cross sections have been presented for a number of processes (total, elastic scattering, momentum transfer, excitation, ionization and electron attachment) [11] to provide benchmark data. There are a few studies on the double differential cross sections (DDCSs) of secondary electrons ejected from CO_2 at intermediate energies in literature [12,13]. The results indicate good agreement between theory and other experimental results. However, significant differences are observed for higher energies [13].

Despite all this work, detailed experimental and theoretical examinations of triple differential cross section (TDCS) for electron-CO_2 collisions have been relatively few. The first experimental (e,2e) study was done by Hussey and Murray [14]. They presented differential ionization cross sections for low-energy electron scattering from the $1\pi_g$ and $4\sigma_g$ orbitals of CO_2 for 10–80-eV incident electron energies in coplanar symmetric (e,2e) experiments. The results were compared with the same energy range results for the diatomic molecule N_2. A double forward peak was observed at low angles and energies for the CO_2 $1\pi_g$ state but not N_2 [14]. TDCSs for CO_2 and N_2 molecules in coplanar asymmetric geometry at incident electron energies around 500–700 eV were measured by Lahmam-Bennani *et al.* [15] for cases corresponding to large momentum transferred to the ion, which yields larger recoil scattering. The experimental data are compared to theoretical calculations using the first Born approximation–two-center continuum (FBA-TCC) approach [16] and the theoretical description was not able to explain the origin of the main structures for the binary and recoil regions.

In this work, we will compare experiment with the two-center Coulomb continuum (TCC) and the molecular three-body distorted wave (M3DW) approximation. Chuluunbaatar and Joulakian extended the TCC model to three centers to obtain a better theoretical description for ionizing linear

*Corresponding author: zehraerengil@aku.edu.tr

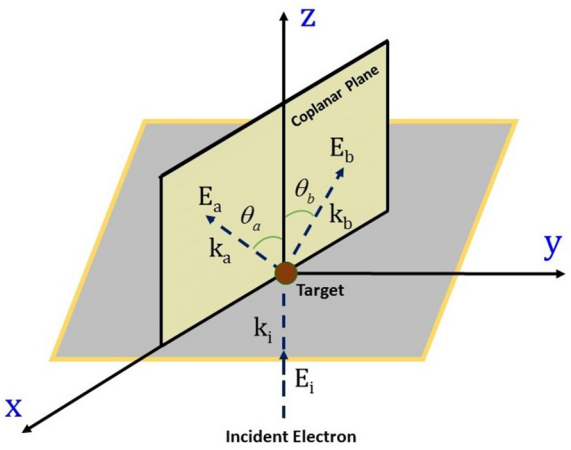

FIG. 1. Schematic drawing of the experimental geometry.

polyatomic targets and used the new model to determine differential cross sections for the outermost and inner shell orbitals of CO_2 [15,17]. We will label this approach as the three-center continuum (ThCC) approximation. The theory was further modified to use Dyson Gaussian orbitals and the results gave better agreement with the experimental data [18].

The M3DW has previously been applied to several molecular targets. A summary of this work up to 2010 was given by Madison and Al-Hagan [19]. More recently, studies have been performed for ionization of CH_4 [20,21], tetrahydrofuran and tetrahydrofuryl [22], NH_3 [23], the cyclic ethers tetrahydrofuran, tetrahydropyran and 1,4-dioxane [24], tetrahydropyran and 1,4-dioxane [25], phenol [26], N_2 [27], ethane [28], and furfural [29]. The M3DW has not been previously applied to CO_2.

In this work, experimental and theoretical coplanar TDCS results will be presented for ionization of the CO_2 $1\pi_g$ state for an incident electron energy of 250 eV, an ejected electron energy of 37 eV, and for three fixed faster electron angles of (10°,20°,30°).

A schematic diagram of the geometry is presented in Fig. 1. The incident electron has energy E_i and momentum k_i, the faster final-state electron is detected at an angle θ_a with energy E_a and momentum k_a, and the slower final-state electron is detected at an angle θ_b with energy E_b and momentum k_b. The momentum transfer direction is defined by

$$\mathbf{q} = \mathbf{k}_i - \mathbf{k}_a. \tag{1}$$

II. EXPERIMENTAL PROCEDURE

The measurements have been carried out using an (e,2e) coincidence spectrometer. The experimental geometry used is coplanar asymmetric geometry, which means that the incident, scattered, and ejected electrons are in a single plane. The scattered electron is detected at a fixed forward angle in coincidence with ejected electron angles ranging from 30° to 130°. The experimental conditions for these measurements were incident electron energy $E_i = 250$ eV, faster final-state electron angle $\vartheta_a = 10°$–$30°$, and slower final-state electron energy $E_b = 37$ eV. The binding energy of the CO_2 $1\pi_g$ orbital is 11.7 eV. The faster final-state electron energy is $E_a = 201.3$ eV, which is determined by energy conservation. Of course, we do not know which electron is the scattered electron and which electron is the ejected electron, but for discussion purposes, we call the faster final-state electron the scattered electron and the slower final-state electron the ejected electron.

Since the apparatus is of a conventional design, only a brief description will be given here. Electrons emitted from a tungsten filament are accelerated and focused to the interaction region to produce a beam of desired energy which can range between 40 and 350 eV by using the electrostatic lenses of an electron gun. The beam is then perpendicularly crossed with the gas beam. The outgoing electrons are energy selected by using two rotatable hemispherical electrostatic energy analyzers at different angles (Fig. 2) and detected by single-channel electron multipliers (CEM) housed on the exit of analyzers. From the width of the peak representing elastically scattered electrons, we determined the spectrometer resolution to be about 0.9 eV FWHM. All the components of the electron spectrometer are housed in a stainless-steel cylindrical vacuum chamber fitted with a μ metal.

The outgoing electrons analyzed with respect to their energies and scattering angles are detected in coincidence. True coincidences are selected by setting conditions on the peak in the coincidence time spectrum. Further experimental details may be found in Refs. [27,30–32].

Using the (e,2e) experimental technique, it is possible to study either the electronic structure of the target or the dynamics of the ionization process. Here we report experiments performed using this setup to study the ionization process of the CO_2 $(1\pi_g)$ orbital. Although there have been a few previous studies of CO_2, there have been no studies in the kinematic range of interest here.

III. THEORETICAL FRAMEWORK

A. Molecular three-body distorted wave

The M3DW approximation has been presented in previous publications [19,21,33], and here we provide only a brief description. The triple differential cross section is given by

$$\frac{d^5\sigma}{d\Omega_a d\Omega_b dE_b} = \frac{1}{(2\pi)^5}\frac{k_a k_b}{k_i}(|T_{\rm dir}|^2 + |T_{\rm exc}|^2 + |T_{\rm dir} - T_{\rm exc}|^2), \tag{2}$$

where $T_{\rm dir}$ and $T_{\rm exc}$ are the direct and exchange scattering amplitudes. The direct amplitude is given by

$$T_{\rm dir} = \langle \chi_a^-(\mathbf{k}_a,\mathbf{r}_0)\chi_b^-(\mathbf{k}_b,\mathbf{r}_1)C_{ab}(\mathbf{r}_{01})|\mathrm{V}_i - U_i|\phi_{Dy}(\mathbf{r}_1,\mathbf{R}) \times \chi_i^+(\mathbf{k}_i,\mathbf{r}_0)\rangle, \tag{3}$$

where $\chi_i^+(\mathbf{k}_i,\mathbf{r}_0)$ is a continuum state distorted for wave, $\chi_a^-(\mathbf{k}_a,\mathbf{r}_0)and\chi_b^-(\mathbf{k}_b,\mathbf{r}_1)$ are the scattered and ejected electron distorted waves, $\phi_{Dy}(\mathbf{r}_1,\mathbf{R})$ is the initial bound-state electronic wave function, commonly called the Dyson molecular orbital for the active electron, which depends both on the spatial coordinate $\mathbf{r}_1$ and the molecular orientation $\mathbf{R}$. The Dyson wave function is defined to be the overlap between the final molecular wave function for the ion and the initial molecular wave function for the neutral molecule. The molecular wave

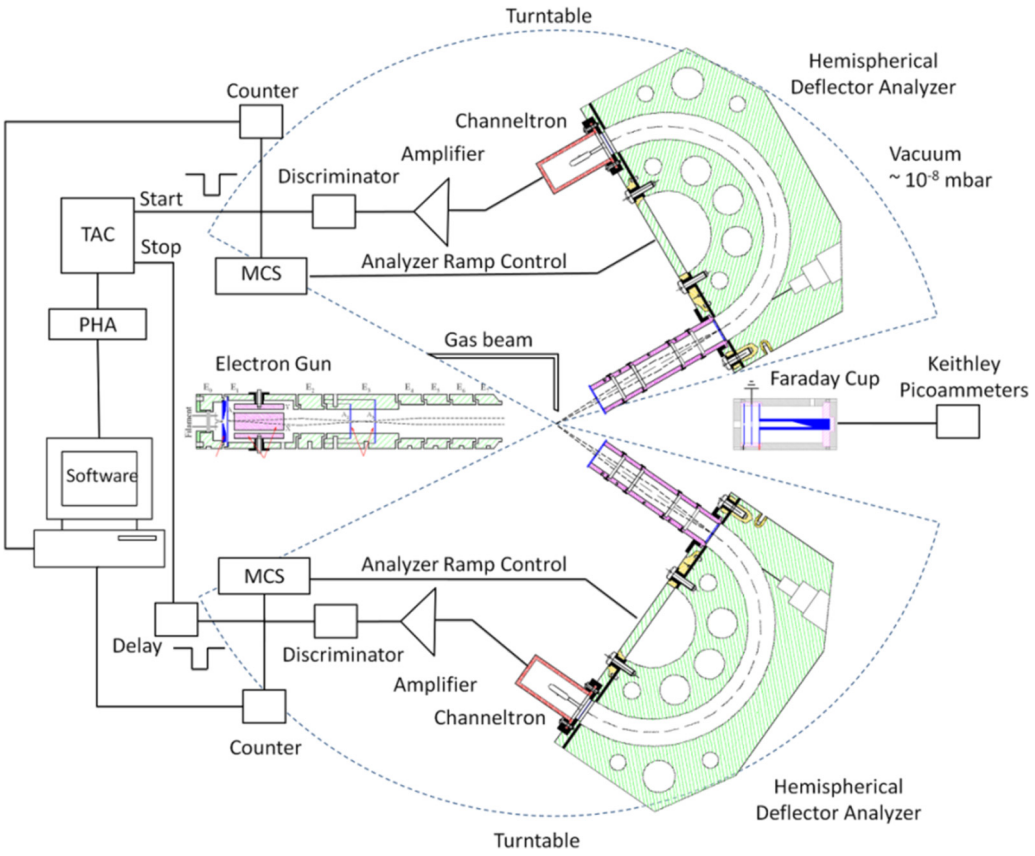

FIG. 2. Schematic view of experimental setup and coincidence electronics.

functions were calculated using density-functional theory along with the standard hybrid B3LYP [34] functional by means of the Amsterdam Density Functional Program ADF 2007 [35] with the TZ2P (triple-zeta with two polarization functions) Slater-type basis sets. The initial-state interaction potential between the projectile and the neutral molecule is V_i, and U_i is a spherically symmetric approximation for V_i. Consequently, V_i–U_i is the nonspherical part of the initial-state projectile-target interaction. The factor $C_{ab}(\mathbf{r}_{01})$ is the final-state Coulomb-distortion factor between the two final-state electrons—normally called the postcollision interaction (PCI). We call results obtained using the above T matrices M3DW (molecular three-body distorted wave). Since the final-state Coulomb interaction is included in the final-state wave function, the M3DW contains PCI to all orders of perturbation theory. The exchange T matrix $T_{\rm exc}$ is the same as Eq. (3), except that $\mathbf{r}_0$ and $\mathbf{r}_1$ are interchanged in the final-state wave function.

The TDCS of Eq. (2) depends on the orientation of the molecule and most experiments do not determine the orientation of the molecule at the time of ionization. Consequently, the theory needs to average over all orientations [20]. To take the average over all molecular orientations, the TDCS is calculated for each orientation and then averaged over all possible orientations so that [to simplify the notation, we label the TDCS of Eq. (2) as $\sigma^{\rm TDCS}(\mathbf{R})$]

$$\sigma^{\rm M3DW} = \frac{\int \sigma^{\rm TDCS}(\mathbf{R}) d\Omega_R}{\int d\Omega_R}. \tag{4}$$

B. Three-center continuum model

We have also used the three-center continuum model with Dyson-type orbitals for the ionization of the $(1\pi_g)$ level of CO_2. In this approach, the TDCS of Eq. (2) is obtained by averaging the multiply differential cross section for fixed orientation of the molecule over all molecular orientations. The orientation of the molecule is given by the polar θ_R and azimuthal φ_R angles defined in the laboratory frame of reference, which has its z axis parallel to the incidence direction of the projectile:

$$\frac{d^5\sigma}{d\Omega_a d\Omega_b dE_b} = \frac{1}{4\pi}\int d\Omega_R \frac{d^7\sigma}{d\Omega_R d\Omega_a d\Omega_b dE_b} \tag{5}$$

with

$$\frac{d^7\sigma}{d\Omega_R d\Omega_a d\Omega_b dE_b} = \frac{k_a k_b}{2k_i}\left[\left|T_{\rm dir}^{m=1}\right|^2 + \left|T_{\rm dir}^{m=-1}\right|^2\right] \tag{6}$$

For the asymmetric regime of the present paper ($E_0 = 250$ eV, $E_b = 37$ eV) we consider only the direct term of the transition matrix element, which is given by

$$T_{\rm dir}^m = \frac{1}{2\pi}\int \overrightarrow{dr_1}\int \overrightarrow{dr_0}\exp i(\vec{k}_i\cdot\vec{r}_0 - \vec{k}_a\cdot\vec{r}_0) \times \chi(\vec{k}_b\cdot\vec{r}_1)V\phi_{1\pi_g}^m(\vec{r}_1). \tag{7}$$

The details concerning the different terms of this expression are given in [17,18]. $\chi(\vec{k}_b\cdot\vec{r}_1)$ represents the three-center continuum function, and $\phi_{1\pi_g}^m(\vec{r}_1)$ is the Dyson orbital [36,37] for the initially bound electron obtained from the coupled cluster results [38,39] by calculating the overlap between the

N state of the target and the (N-1) state of the ionized ion. V represents the model potential describing the interaction of the incident electron with the target.

IV. RESULTS

The M3DW has yielded reasonably good agreement with experiment for several different molecular targets but it has not been previously applied to CO_2. In the past, the two-center Coulomb continuum model, which applies two-center Coulomb continuum functions obtained from the solution of the Schrödinger equation for a free electron in the Coulomb field of two fixed charged nuclei, was extended to three-center targets (ThCC) and has been applied to the ionization of CO_2 [17] for higher incident (∼500 eV) energy asymmetric cases. In Ref. [18], it was slightly modified by the introduction of a supplementary parameter, which adds some flexibility to the function and adapts it to more general situations. Five types of calculations were done, with different model potential parameters for the interaction of the incident electron with the target. In this work, we will consider type 5, which takes into account all the screening of the inactive electrons of the target borrowed from Ref. [40]. The electronic structure of CO_2 is described by Dyson orbitals. To avoid cumbersome calculations, the incident and scattered electrons, at this stage, are described by plane waves. We think that for the incident energy domain (250 eV) of the present experiment, this could be considered as a compromise, which should be improved in the future.

The present M3DW model contains the postcollision interaction (PCI) between scattered and ejected electrons to all orders of perturbation theory, which has been shown to be very important for several other cases. In the M3DW model, the in- and outgoing electrons are described by a wave distorted by the perturbing potential, i.e., the interaction with the target. With the inclusion of PCI, TDCS can be calculated that agree reasonably well with experiments down to relatively low impact energies. There are no adjustable parameters in the M3DW.

The aim of this work is to compare experimental and theoretical results for (e,2e) ionization of CO_2 for intermediate energies. From previous works for ionization, it has been found that the typical (e,2e) coplanar cross sections have a large peak in the forward direction. This peak is called the binary peak since it is close to the direction that a classical particle would leave a collision for elastic scattering of two equal mass particles (the momentum transfer direction $+\mathbf{q}$). Also, typically there is a much smaller peak at large angles, which is normally close to 180° from the binary peak (the negative of the momentum transfer direction $-\mathbf{q}$) and this small peak is called the recoil peak since it is attributed to a binary electron being backscattered from the nucleus. Figure 3 shows the CO_2 $1\pi_g$ orbital. It is seen that it has the appearance of two atomic p-type states. It is also known that for an atomic p state, the binary peak often is split into two peaks with a minimum at the direction of momentum transfer.

Figure 4 shows the comparison of the experimental results with the predictions of the M3DW and ThCC (type 5) models. Since the experimental data are not absolute, the experiment is normalized to the M3DW at the binary peak. The ThCC model predicts cross sections a little larger than the M3DW for all the cases we considered. Consequently, we multiplied the ThCC results by 0.8 so that the theoretical cross sections have the same magnitude for the largest cross section ($\theta_a = 10°$ binary peak). It is seen that both experiment and theory predict a

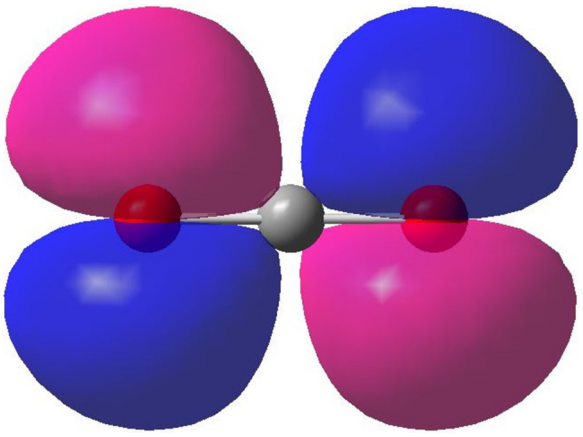

FIG. 3. The $CO_2 1\pi_g$ orbital. The center small ball is the carbon atom, the two balls on either side are the oxygen atoms, and the larger oval shapes are the electron wave function of either positive or negative sign.

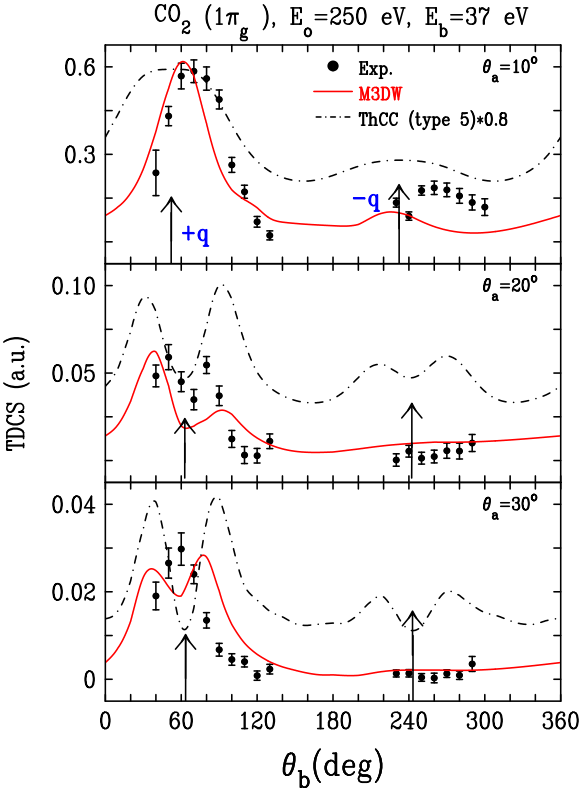

FIG. 4. TDCS in atomic units (a.u.) for electron-impact ionization of the $1\pi_g$ state of CO_2 plotted as a function of the ejection angle for the 37-eV ejected electron. The experimental results are normalized to the M3DW calculations at the binary peak. The arrow near 60° is the momentum transfer direction ($+\mathbf{q}$) and the arrow near 240° is the negative momentum transfer direction ($-\mathbf{q}$).

single binary peak at $\theta_a = 10^\circ$ and a double binary peak at $\theta_a = 20^\circ$, which is a known characteristic for ionization of atomic p states. The ThCC predicts the relative heights of the two peaks better than the M3DW at 20°. However, for $\theta_a = 30^\circ$, both theories predict a double peak while experiment only has a single peak. Also shown in Fig. 4 is the location of the momentum transfer ($+\mathbf{q}$) and location of the expected recoil peak ($-\mathbf{q}$). It is seen that, at $\theta_a = 10^\circ$, the experiment and M3DW have binary peaks at a larger angle than the momentum transfer, which would be attributed to PCI.

The similarity of the present results and atomic p-type cross sections is further enhanced by noting that, in both experiment and theory, single peaks occur near the momentum transfer direction and, for double peaks, the minimum between the two peaks occurs near the momentum transfer direction, which is the same as the atomic case. There have been several papers published for ionization of argon $3p$ for similar kinematics [31,41–44]. For 10° scattering, all theories and experiment had a single binary peak for ejected electron energies above 10 eV, which is consistent with the present results. For 20° scattering, all theories and experiment indicated a double peak again similar to the present case. Unfortunately, we could not find any 30° measurements, which is disappointing since it would be very interesting to see if other works found a single peak or double peak for 30°. To our knowledge, a way to predict when to expect a single or double peak has not been found.

For this kinematics, there is almost no recoil peak in the experimental data except for a slight hint that there might be a small one for $\theta_a = 10^\circ$ but at angles larger than the expected recoil peak location. The ThCC predicts a very broad recoil-type peak that is qualitatively in agreement with experiment at $\theta_a = 10^\circ$ while the M3DW predicts a very small peak near the expected recoil peak location. For $\theta_a = 20^\circ$and30°, the ThCC predicts a double recoil peak with a minimum at $-\mathbf{q}$, and the magnitude is much larger than the data. For $\theta_a = 20^\circ$ and 30°, the M3DW and experimental data have very small cross sections in the recoil region.

As can be seen from the figure, there is qualitative agreement between theory and experiment. The ThCC qualitatively predicts the shape of the binary peak for $\theta_a = 10^\circ$and20° but not $\theta_a = 30^\circ$, and it predicts a larger cross section than seen in experiment for the two larger scattering angles. The M3DW gives the best overall agreement with data except for predicting a double binary peak at $\theta_a = 30^\circ$.

V. CONCLUSION

The scattering of electrons by a polyatomic linear molecular target is one of the basic problems in molecular collisions. There have been a limited number of (e,2e) studies for electron-impact ionization of CO_2 but none for the intermediate kinematics examined here. In this work, we compared experiment and theory for intermediate-energy electron-impact ionization of the $1\pi_g$ state of CO_2. The $1\pi_g$ state has the shape of a double atomic p state, which typically can have a double binary peak (but not always) with the minimum located near the momentum transfer direction. We compared M3DW and ThCC (type 5) theoretical results with experimental data and found p-state evidence in the binary peak both experimentally and theoretically. Both the ThCC and M3DW predicted a double-peak structure for both the two larger scattering angles, while experiment found a double peak for the middle angle only. There was an indication of a recoil peak only for the smallest projectile scattering angle. The M3DW was in the best overall agreement with experiment, except for the prediction of a double binary peak for the largest projectile scattering angle.

ACKNOWLEDGMENTS

This work was supported by the Scientific and Technological Research Council of Turkey (TUBITAK) through Grant No. 109T738 and by BAPK through Grant No. 15.HIZ.DES.130, 14FENED.06. E.A. and D.M. would like to acknowledge the support of the US National Science Foundation under Grant. No. PHY-1505819 and C.N. would like to acknowledge the support of the National Natural Science Foundation of China under Grant No. 11174175. Computational work was performed with Institutional Computing resources made available through the Los Alamos National Laboratory. The Los Alamos National Laboratory is operated by Los Alamos National Security, LLC, for the National Nuclear Security Administration of the US Department of Energy under Contract No. DE-AC5206NA25396.

[1] H. Tanaka, T. Ishikawa, T. Masai, T. Sagara, L. Boesten, M. Takekawa, Y. Itikawa, and M. Kimura, Phys. Rev. A **57**, 1798 (1998).

[2] M. Kimura, M. Inokuti, K.-I. Kowari, M. A. Dillon, and A. Pagnamenta, Radiat. Phys. Chem. **34**, 481 (1989).

[3] T. Shirai, T. Tabata, and H. Tawara, At. Data Nucl. Data Tables **79**, 143 (2001).

[4] G. P. Karwasz, R. S. Brusa, and A. Zecca, Riv. Nuovo Cimento Soc. Ital. Fis. **24**, 1 (2001).

[5] G. N. Ogurtsov, J. Phys. B: At., Mol. Opt. Phys. **28**, 1805 (1998).

[6] D. F. Register, H. Nishimura, and S. Trajmar, J. Phys. B: At., Mol. Opt. Phys. **13**, 1651 (1980).

[7] T. W. Shyn, W. E. Sharp, and G. R. Carignan, Phys. Rev. A **17**, 1855 (1978).

[8] R. McDiarmid and J. P. Doering, J. Chem. Phys. **80**, 648 (1984).

[9] K. Anzai, H. Kato, M. Hoshino, H. Tanaka, Y. Itikawa, L. Campbell, M. J. Brunger, S. J. Buckman, H. Cho, F. Blanco, G. Garcia, P. Limão-Vieira, and O. Ingólfsson, Eur. Phys. J. D **66**, 36 (2012).

[10] M. A. Green, P. J. O. Teubner, L. Campbell, M. J. Brunger, M. Hoshino, T. Ishikawa, M. Kitajima, H. Tanaka, Y. Itikawa, M. Kimura, and R. J. Buenker, J. Phys. B: At. Mol. Opt. Phys. **35**, 567 (2002).

[11] Y. Itikawa, J. Phys. Chem. Ref. Data **31**, 749 (2002).

[12] T. W. Shyn and W. E. Sharp, Phys. Rev. A **20**, 2332 (1979).

[13] C. B. Opal, W. K. Peterson, and E. C. Beaty, J. Chem. Phys. **55**, 4100 (1971).

[14] M. J. Hussey and A. J. Murray, J. Phys. B: At., Mol. Opt. Phys. **38**, 2965 (2005).
[15] A. Lahmam-Bennani, E. M. Staicu Casagrande, and A. Naja, J. Phys. B: At., Mol. Opt. Phys. **42**, 235205 (2009).
[16] B. Joulakian, J. Hanssen, R. Rivarola, and A. Motassim, Phys. Rev. A **54**, 1473 (1996).
[17] O. Chuluunbaatar and B. Joulakian, J. Phys. B: At., Mol. Opt. Phys. **43**, 155201 (2010).
[18] O. Alwan, O. Chuluunbaatar, X. Assfeld, A. Naja, and B. Joulakian, J. Phys. B: At., Mol. Opt. Phys. **47**, 225201 (2014).
[19] D. H. Madison and O. Al-Hagan, J. At. Mole. Opt. Phys. **2010**, 1 (2010).
[20] S. Xu, Hari Chaluvadi, X. Ren, T. Pflüger, A. Senftleben, C. G. Ning, S. Yan, P. Zhang, J. Yang, X. Ma, J. Ullrich, D. H. Madison, and A. Dorn, J. Chem. Phys. **137**, 024301 (2012).
[21] H. Chaluvadi, C. G. Ning, and D. Madison, Phys. Rev. A **89**, 062712 (2014).
[22] D. Jones, J. D. Builth-Williams, S. M. Bellm, L. Chiari, H. Chaluvadi, D. Madison, C. Ning, B. Lohmann, O. Ingólfsson, and M. Brunger, Chem. Phys. Lett. **572**, 32 (2013).
[23] K. L. Nixon, A. J. Murray, H. Chaluvadi, C. Ning, J. Colgan, and D. H. Madison, J. Chem. Phys. **138**, 174304 (2013).
[24] J. D. Builth-Williams, S. M. Bellm, L. Chiari, P. A. Thorn, D. B. Jones, H. Chaluvadi, D. H. Madison, C. G. Ning, B. Lohmann, G. da Silva, and M. J. Brunger, J. Chem. Phys. **139**, 034306 (2013).
[25] J. D. Builth-Williams, G. B. da Silva, L. Chiari, D. B. Jones, H. Chaluvadi, D. H. Madison, and M. J. Brunger, J. Chem. Phys. **140**, 214312 (2014).
[26] G. B. da Silva, R. F. C. Neves, L. Chiari, D. B. Jones, E. Ali, D. H. Madison, C. G. Ning, K. L. Nixon, M. C. A. Lopes, and M. J. Brunger, J. Chem. Phys. **141**, 124307 (2014).
[27] H. Chaluvadi, Z. N. Ozer, M. Dogan, C. Ning, J. Colgan, and D. Madison, J. Phys. B **48**, 155203 (2015).
[28] E. Ali, K. Nixon, A. Murray, C. Ning, J. Colgan, and D. Madison, Phys. Rev. A **92**, 042711 (2015).
[29] D. B. Jones, E. Ali, K. L. Nixon, P. Limão-Vieira, M.-J. Hubin-Franskin, J. Delwiche, C. G. Ning, J. Colgan, A. J. Murray, D. H. Madison, and M. J. Brunger, J. Chem. Phys. **143**, 184310 (2015).
[30] Z. N. Ozer, H. Chaluvadi, M. Ulu, M. Dogan, B. Aktas, and D. Madison, Phys. Rev. A **87**, 042704 (2013).
[31] S. Amami, M. Ulu, Z. N. Ozer, M. Yavuz, S. Kazgoz, M. Dogan, O. Zatsarinny, K. Bartschat, and D. Madison, Phys. Rev. A **90**, 012704 (2014).
[32] M. Dogan, M. Ulu, Z. N. Ozer, M. Yavuz, and G. Bozkurt, J. Spectrosc. **2013**, 1 (2013).
[33] J. Gao, D. H. Madison, and J. L. Peacher, J. Chem. Phys. **123**, 204302 (2005).
[34] C. F. Guerra, J. G. Snijders, G. Te Velde, and E. J. Baerends, Theor. Chem. Acc. **99**, 391 (1998).
[35] C. Lee, W. Yang, and R. G. Parr, Phys. Rev. B **37**, 785 (1988).
[36] I. G. Kaplan, B. Barbiellini, and A. Bansil, Phys. Rev. B **68**, 235104 (2003).
[37] R. J. F. Nicholson, I. E. McCarthy, and W. Weyrich, J. Phys. B: At., Mol. Opt. Phys. **32**, 3873 (1999).
[38] C. M. Oana and A. I. Krylov, J. Chem. Phys. **127**, 234106 (2007).
[39] C. M. Oana and A. I. Krylov, J. Chem. Phys. **131**, 1241143 (2009).
[40] F. J. Rogers, B. G. Wilson, and C. A. Iglesias, Phys. Rev. A **38**, 5007 (1988).
[41] M. Stevenson, G. J. Leighton, A. Crowe, K. Bartschat, O. K. Vorov, and D. H. Madison, J. Phys. B: At., Mol. Opt. Phys. **40**, 1639 (2007).
[42] X. Ren, A. Senftleben, T. Pflueger, A. Dorn, K. Bartschat, and J. Ullrich, J. Phys. B: At., Mol. Opt. Phys. **43**, 035202 (2010).
[43] Xueguang Ren, Arne Senftleben, Thomas Pflueger, Alexander Dorn, Klaus Bartschat, and Joachim Ullrich, Phys. Rev. A **83**, 052714 (2011).
[44] M. Ulu, Z. N. Ozer, M. Yavuz, O. Zatsarinny, K. Bartschat, M. Dogan, and A. Crowe, J. Phys. B: At., Mol. Opt. Phys. **46**, 115204 (2013).